

SPECIALIST PERIODICAL REPORTS

Catalysis

VOLUME 9

ROYAL SOCIETY OF CHEMISTRY

Catalysis

Volume 9

A Review of Recent Literature

Senior Reporter

J.J. Spivey, *Center for Process Research, Research Triangle Institute, North Carolina, USA*

Reporters

G. Cinquegrane, *Burns and Roe Services Corporation, Pittsburgh, PA, USA*

W.C. Conner, *University of Massachusetts, Amherst, MA, USA*

D.B. Dadyburjor, *West Virginia University, Morgantown, WV, USA*

W.J.H. Dehertog, *Rijksuniversiteit Gent, Belgium*

J.W. Eldridge, *University of Massachusetts and KSE Inc., Amherst, MA, USA*

N.S. Figoli, *INCAPE, Santa Fe, Argentina*

G.F. Froment, *Rijksuniversiteit Gent, Belgium*

J.R. Kittrell, *KSE Inc., Amherst, MA, USA*

A.J. Marchi, *Rijksuniversiteit Gent, Belgium*

J.M. Parera, *INCAPE, Santa Fe, Argentina*

V.U.S. Rao, *Burns and Roe Services Corporation, Pittsburgh, PA, USA*

R.D. Srivastava, *Burns and Roe Services Corporation, Pittsburgh, PA, USA*

G.J. Stiegel, *Burns and Roe Services Corporation, Pittsburgh, PA, USA*

P. Zhou, *Burns and Roe Services Corporation, Pittsburgh, PA, USA*

ISBN 0-85186-604-2

Copyright © 1992
The Royal Society of Chemistry

All Rights Reserved

No part of this book may be reproduced or transmitted in any form or by any means—graphic, electronic, including photocopying, recording, taping, or information storage and retrieval systems—without written permission from The Royal Society of Chemistry

Published by The Royal Society of Chemistry,
Thomas Graham House, Science Park, Cambridge CB4 4WF

Printed and bound in Great Britain by Bookcraft (Bath) Ltd

Catalysis

Volume 9

Preface

This volume of the Specialist Periodical Reports in Catalysis continues the work of bringing to the reader current reviews on a range of subjects. I am indebted to Professors G. C. Bond and G. Webb for their efforts in preparing the volumes immediately preceding this one and hope to continue to bring to you topics of general interest. I also greatly appreciate the help of my colleague Dr. Sanjay K. Agarwal, who provided review of several manuscripts and useful suggestions on their organization and content.

Three of the five reviews in this current volume deal with the subject of deactivation. I cannot claim that this was done by design, however. This reflects, it appears, a somewhat general interest in deactivation, perhaps catalyzed by the recent Fifth International Symposium on Catalyst Deactivation at Northwestern University (C. H. Bartholomew and J. B. Butt, Chairmen).

In the first chapter, Professor Froment and his colleagues W. J. H. Dehertog and A. J. Marchi at Rijksuniversiteit Gent (Belgium) provide a comprehensive review of zeolite catalysis for the methanol-to-olefin reaction. He examines small, medium, and large-pore zeolites, the important role of acidity and shape selectivity on product distribution, and, like several of the other Reporters, the importance of understanding the coke-forming deactivation processes.

Professors Parera and Fígoli continue their important work at INCAPE (Santa Fe, Argentina) on naphtha reforming by presenting a discussion of deactivation on dual-function catalysts. Their work covers coking, poisoning, and sintering as well as regeneration techniques.

Dr. Jim Kittrell and J. W. Eldridge at KSE, Inc. (Amherst, MA) and Professor W. C. Conner (University of Massachusetts) report on deactivation of stationary source emission control catalysts. In addition to a general discussion of deactivation and ways to characterize it, they focus on the important applications of NO_x reduction and control of volatile organic compounds, both of which are receiving increased regulatory attention.

Extensive reserves of natural gas in the United States and elsewhere have made the catalytic conversion of methane to liquid fuels and chemicals an important topic for research. Drs. R. D. Srivastava and Pei Zhou at Burns and Roe (Pittsburgh, PA), together with G. J. Stiegel, Dr. V. U. S. Rao, and G. J. Cinquegrane at the U. S. Department of Energy, discuss the leading candidate processes and their respective costs.

Finally, Professor Dadyburjor at West Virginia University gives a thorough overview of the effect of various processes, which collectively constitute observable deactivation, on selectivity. He examines a wide range of reactions and catalysts with this unifying theme.

It has been my pleasure to work with the Reporters contributing to Volume 9 of this series. Over the past year since work began on this volume, I have had the opportunity to meet each lead Reporter either at technical conferences or here at the Institute. Work has already begun on Volume 10, which will be ready in about a year. Comments on the current volume and suggestions for future volumes are welcome.

J. J. Spivey
Research Triangle Institute
Research Triangle Park, NC

Contents

Chapter 1 Zeolite Catalysis in the Conversion of Methanol into Olefins

By G.F. Froment, W.J.H. Dehertog, and A.J. Marchi

| | | |
|-------|---|----|
| 1 | Introduction | 1 |
| 2 | Small-pore Molecular Sieves | 2 |
| 2.1 | Principal Characteristics | 2 |
| 2.2 | Methanol Conversion to Olefins | 7 |
| 2.3 | Deactivation by Coke | 18 |
| 3 | Medium-pore Zeolites | 20 |
| 3.1 | Principal Characteristics | 20 |
| 3.1.1 | Structure | 20 |
| 3.1.2 | Acidity | 22 |
| 3.1.3 | Shape Selectivity | 24 |
| 3.2 | Methanol Conversion to Olefins on ZSM-5 | 24 |
| 3.2.1 | Influence of Space Time | 24 |
| 3.2.2 | Influence of Si/Al-ratio | 26 |
| 3.2.3 | Influence of the Temperature | 27 |
| 3.2.4 | Influence of Partial Pressure | 29 |
| 3.2.5 | Influence of Catalyst Preparation | 32 |
| 3.3 | Methanol Conversion to Olefins on Modified ZSM-5 | 33 |
| 3.3.1 | Ion-exchange and Impregnation | 33 |
| 3.3.2 | Isomorphous Substitution of Si | 36 |
| 3.4 | Conversion of Methanol on Other Medium-pore Zeolites | 38 |
| 3.5 | Deactivation and Coke Formation on Medium-pore Zeolites | 41 |
| 4 | Large-pore Molecular Sieves | 44 |
| 4.1 | Principal Characteristics | 44 |
| 4.2 | Methanol Conversion to Olefins | 46 |
| 4.3 | Deactivation by Coke | 52 |
| 5 | Reaction Mechanism and Kinetics | 54 |
| | References | 59 |

Chapter 2 Deactivation and Regeneration of Naphtha Reforming Catalysts

By J.M. Parera and N.S. Figoli

| | | |
|-------|--|-----|
| 1 | Introduction | 65 |
| 2 | Deactivation | 67 |
| 2.1 | Deactivation by Coking | 68 |
| 2.1.1 | Coke Deposition on the Catalytic Functions and their Deactivations | 69 |
| 2.1.2 | Influence of Catalyst Composition | 80 |
| | Influence of the Metal Function | 80 |
| | Influence of the Acid Function | 85 |
| 2.1.3 | Influence of Operating Conditions | 90 |
| 2.1.4 | Influence of Feed Composition | 93 |
| 2.2 | Deactivation by Poisoning | 98 |
| 2.2.1 | Deactivation by Sulfur Compounds | 98 |
| 2.2.2 | Deactivation by Nitrogen Compounds | 104 |
| 2.3 | Deactivation by Sintering | 106 |
| 2.3.1 | Sintering of the Metal Function | 106 |
| | Influence of Temperature and Atmosphere | 106 |
| | Influence of Support and Time | 109 |
| | Influence of a Second Metal | 110 |
| 2.3.2 | Sintering of the Acid Function | 112 |
| 2.4 | Deactivation by Chloride Elimination | 113 |
| 3 | Regeneration | 114 |
| 3.1 | Coke Elimination by Burning | 114 |
| 3.2 | Elimination of Sulfur | 116 |
| 3.3 | Redispersion of the Metal Function and Chloride Adjustment | 119 |
| | References | 122 |

Chapter 3 Deactivation of Stationary Source Air Emissions Control Catalysts

By J.R. Kittrell, J.W. Eldridge, and W.C. Conner

| | | |
|-------|---|-----|
| 1 | Introduction | 126 |
| 1.1 | Background | 126 |
| 1.2 | Deactivation Mechanisms | 126 |
| 1.3 | Reversible/Irreversible Poisoning | 130 |
| 2 | Morphological Changes during Deactivation | 135 |
| 2.1 | Morphological Characteristics and Their Measurement | 135 |
| 2.2 | Morphological Changes in VOC and SCR Catalysts | 136 |
| 2.2.1 | Global Changes in Morphology for Oxide Catalysts | 137 |

| | | |
|------------------|--|-----|
| 2.2.2 | Phase Transitions in Metal Oxide Catalysts | 140 |
| 2.2.3 | Sintering of Supported Metals | 141 |
| 2.3 | Summary of Morphological Changes during Deactivation | 142 |
| 3 | Deactivation of NO _x Reduction Catalysts | 144 |
| 3.1 | Effects of Sulfur | 144 |
| 3.2 | Effects of Alkali and Alkaline Earth Metal Oxides and Salts | 153 |
| 3.3 | Effects of Arsenic and Other Heavy Metals | 156 |
| 3.4 | Effects of Fly Ash Metals | 158 |
| 3.5 | Deactivation by Soot and Fly Ash Deposition | 159 |
| 3.6 | Thermal Deactivation | 159 |
| 4 | Oxidation Catalysts for Non-halogenated VOCs | 160 |
| 4.1 | Effects of Sulfur | 160 |
| 4.2 | Effects of Halogens | 163 |
| 4.3 | Effects of Phosphorus and Heavy Metals | 166 |
| 4.4 | Effects of Deposits on the Catalysts | 166 |
| 4.5 | Thermal Deactivation | 167 |
| 5 | Halogenated Hydrocarbon Oxidation Catalysts | 167 |
| 6 | Detailed Characterization of Deactivation | 170 |
| 6.1 | Morphological Changes | 171 |
| 6.2 | Deposition of Poisons | 172 |
| 6.3 | Specific Site Poisoning | 173 |
| 6.4 | Solid State Transformations | 173 |
| 6.5 | Potential Use of Detailed Characterization Techniques | 174 |
| | References | 175 |
| Chapter 4 | Direct Conversion of Methane to Liquid Fuels and Chemicals | |
| | <i>By R.D. Srivastava, P. Zhou, G.J. Stiegel, V.U.S. Rao, and G. Cinquegrane</i> | |
| 1 | Introduction | 183 |
| 2 | Thermodynamic and Kinetic Considerations | 184 |
| 3 | Methane Conversion Technologies: Literature Review | 188 |
| 3.1 | Direct Partial Oxidation to Methanol | 188 |
| 3.1.1 | Using Oxygen | 188 |
| 3.1.2 | Using Nitrous Oxide | 189 |
| 3.1.3 | Homogeneous Gas-Phase Oxidation | 190 |
| 3.2 | Oxidative Coupling to Ethylene | 191 |
| 3.2.1 | An Overview | 193 |
| 3.2.2 | Review of Published Results and Patent Literature | 193 |

| | | |
|------------------|--|-----|
| 3.2.3 | Other Promising Oxidative Coupling Processes | 204 |
| 3.3 | Oxyhydrochlorination/Oxychlorination | 205 |
| 3.4 | Superbiotic Catalyst Systems | 208 |
| 3.5 | Other Direct Conversion Processes | 210 |
| 4 | Economic Assessment | 212 |
| 4.1 | Economic Evaluation (Methane to Liquid Hydrocarbon Fuels) | 212 |
| 4.2 | Oxidative Coupling | 213 |
| 4.3 | Partial Oxidation to Methanol | 213 |
| 4.4 | Oxyhydrochlorination | 215 |
| 4.5 | Study Basis | 215 |
| 4.6 | Summary of Economic Results | 219 |
| 5 | Technology Status and Conclusions | 221 |
| 5.1 | Oxyhydrochlorination | 221 |
| 5.2 | Oxidative Coupling | 221 |
| 5.3 | Partial/Selective Oxidation | 221 |
| 5.4 | Novel Catalysts | 222 |
| 5.5 | Concluding Remarks | 222 |
| | References | 222 |
| Chapter 5 | Effect of Deactivation on Catalyst Selectivity <i>By D.B. Dadyburjor</i> | |
| 1 | Introduction | 229 |
| 1.1 | Definitions | 229 |
| 1.2 | Catalysts | 231 |
| 1.3 | Reaction Analysis | 233 |
| 1.3.1 | Hydrogenolysis | 233 |
| 1.3.2 | Isomerization | 235 |
| 1.3.3 | Cracking | 235 |
| 1.4 | Reactors | 236 |
| 2 | Surface Techniques in Deactivation | 238 |
| 2.1 | 'Pressure-gap' Reactors | 239 |
| 2.2 | Coke Characterization | 240 |
| 2.3 | Poison Characterization | 241 |
| 2.4 | Sintering | 242 |
| 3 | Models | 242 |
| 3.1 | Phenomenological Models | 242 |
| 3.2 | Physical Models | 244 |
| 4 | Zeolite Catalysts | 246 |
| 4.1 | Pretreatment Effects | 246 |
| 4.2 | Effects of Coke and Poison on Ring Compounds | 249 |

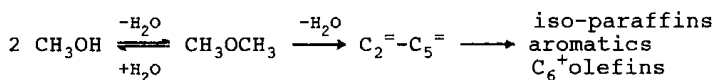
| | | |
|-----|--|-----|
| 4.3 | Effects of Coke and Poison on Straight-chain Compounds | 253 |
| 4.4 | Effects of Coke and Poison on Gasoline Selectivity | 257 |
| 5 | Supported Metal Catalysts | 260 |
| 5.1 | Particle Size Effect | 260 |
| 5.2 | Coke Effect | 265 |
| 5.3 | Support Effect | 267 |
| 5.4 | Second Metal Effect | 269 |
| 5.5 | Effect of Pretreatments and Poisons | 272 |
| 6 | Summary and Conclusions | 275 |
| | References | 276 |

Zeolite Catalysis in the Conversion of Methanol into Olefins

BY G.F. FROMENT, W.J.H. DEHERTOG, AND A.J. MARCHI

1 Introduction

Light olefins are key components in the petrochemical industry. Conventionally, they are produced by thermal cracking of naphtha. The importance of the research efforts to viable routes in the production of basic chemicals, independent of oil, cannot be overlooked. Methanol, which can readily be produced from coal or natural gas via synthesis gas ($\text{CO} + \text{H}_2$) by existing and proven technologies, offers an interesting alternative.¹⁻³ Although methanol itself is a potential motor fuel or can be blended with gasoline, it would require large investments to overcome the technical problems associated with it. Mobil's announcement of a zeolite-based process for the conversion of methanol into gasoline^{1,4,5} provided a new route for the conversion of coal to gasoline. This methanol-to-gasoline (MTG) process was based on a new class of synthetic shape-selective zeolites⁶ differing from the classical small-pore and large-pore zeolites in their pore dimensions, which are intermediate, and their Si/Al-ratio, which can be very high. An excellent review on the MTG-process is given by Chang.⁷ The general reaction path of the methanol conversion to hydrocarbons is:^{8,9}



Methanol is first dehydrated to dimethylether (DME). The equilibrium mixture thereof is then converted to light olefins. In the final steps of the reaction path, the $\text{C}_2\text{-C}_5$ olefins are converted to paraffins, aromatics, naphthenes and higher olefins by polycondensation and alkylation reactions. The importance of light olefins as intermediates in the conversion of methanol to gasoline was soon recognized. As a result, several attempts were made to selectively produce light olefins from methanol on zeolite catalysts, not only on medium-pore zeolites but also on small-pore

and, to a lesser extent, on large-pore zeolites. The development of a new type of molecular sieve (silico-alumino-phosphates)¹⁰ with a zeolite-like framework structure offered interesting perspectives in the methanol conversion to olefins.¹¹ This review describes and compares the various zeolitic catalysts and operational conditions that have been reported to influence the olefin selectivity in the methanol-to-olefins (MTO) process. The reaction mechanism, which has already been reviewed extensively, will be dealt with briefly.

2 Small-pore Molecular Sieves

2.1 Principal Characteristics. - Molecular sieves with pore openings of about 0.45 nm show very interesting shape-selectivity properties for the conversion of methanol to olefins (MTO process). The small-pore molecular sieves studied in the MTO process are chabazite, erionite, zeolite T, ZK-5, ZSM-34, zeolite A, SAPO-17, SAPO-34, and SAPO-44. All of them can sorb only straight chain molecules, e.g. primary alcohols and linear paraffins and olefins, but no branched isomers and aromatics: the pore opening is smaller than the kinetic diameter of branched and aromatic molecules, but large enough to permit the access of linear molecules.

The pore openings of small-pore molecular sieves are 8-membered oxygen rings. The dimensions vary with the shape of the rings, but the effective size is always lower than 0.45 nm. The ring shape may be circular or puckered and elliptical (see Table 1).

The porous systems of small-pore molecular sieves are conformed by ellipsoidal or spherical cavities that share the 8-membered oxygen rings to generate a three-dimensional channel system. These

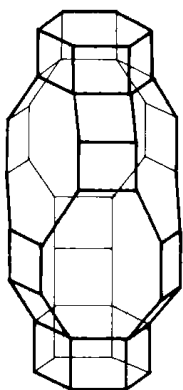
Table 1 Principal characteristics of pore structure for some small-pore molecular sieves^{12,13}

| Name | Ring shape | Pore size (nm) | Cavity shape | Cavity size (nm) |
|-----------|------------|-------------------|--------------|---------------------|
| Chabazite | Elliptical | 0.42x0.37 | Ellipsoidal | 0.65x1.10 |
| Erionite | Elliptical | 0.35x0.52 | Ellipsoidal | 0.66x1.51 |
| Zeolite A | Circular | 0.42 | Spherical | 1.14 |

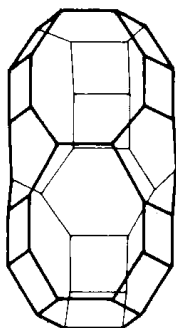
cages are normally much larger than the connecting windows (see Table 1). The structures of chabazite, erionite, and zeolite A cavities are shown in Figure 1.

Chabazite^{12,13} has a rhombohedral symmetry and its typical composition in the hydrated form is $(\text{Ca}, \text{Na}_2)\text{O} \cdot \text{Al}_2\text{O}_3 \cdot 4\text{SiO}_2 \cdot 6-6.5\text{H}_2\text{O}$. Its framework consists of double-6-rings (D6R) arranged in layers in the sequence ABCABC. The hexagonal prisms formed in this way are linked by tilted 4-membered rings (see Figure 1(a)). The resulting framework possesses large, ellipsoidal cages composed of D6R at top and bottom, six 8-rings in rhombohedral positions and six pairs of adjacent 4-rings. The cavities are interconnected to six others by the puckered elliptical 8-rings.

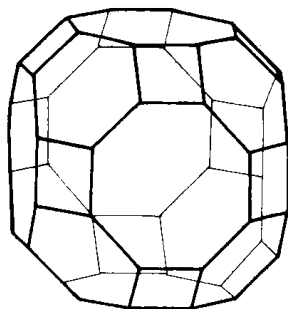
Erionite^{12,13} has a hexagonal symmetry and its typical formula can be written as $(\text{Ca}, \text{Mg}, \text{Na}_2, \text{K}_2)\text{O} \cdot \text{Al}_2\text{O}_3 \cdot 6\text{SiO}_2 \cdot 6\text{H}_2\text{O}$. Its framework consists of D6R units, arranged in the sequence AABAAC. These hexagonal prisms are linked by 4-rings and single 6-rings (cancrinite cages). The structure contains "supercages" that are supported by the columns formed by cancrinite units and the hexagonal prisms (see Figure 2). The result is a complex pore system interconnected by the 8-rings. The sorption cavity is the "supercage". Molecules have access to this cavity through the six elliptical openings formed by 8-rings.



(a) chabazite

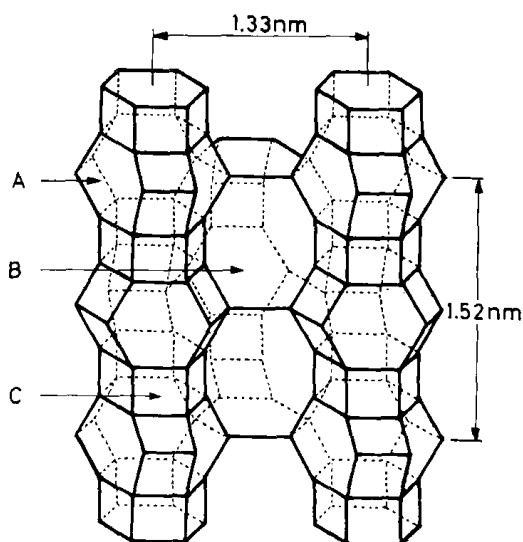


(b) erionite



(c) zeolite A

Figure 1 Cavities of chabazite, erionite, and zeolite A.



A = cancrinite
 B = supercage
 C = hexagonal prism

Figure 2 Erionite framework.

Zeolite A has a cubic symmetry and its typical formula is $\text{Na}_2\text{O} \cdot \text{Al}_2\text{O}_3 \cdot 2\text{SiO}_2 \cdot 4.5\text{H}_2\text{O}$. Its framework can be understood as truncated octahedral units linked by D4R units (see Figure 3). The result is a large spherical cavity with twelve 4-rings, eight 6-rings, and six 8-rings. The three-dimensional porous structure is originated by the linkage of the large cavities through the 8-rings.

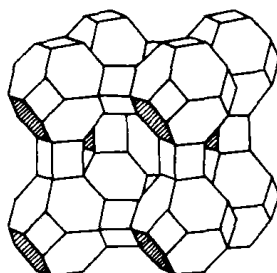
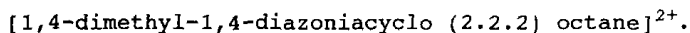


Figure 3 Zeolite A framework.

ZK-5 structure is close to that of zeolite A. It consists of truncated cuboctahedra linked by D6R units. Its typical formula^{12,13} is $(R, Na_2)O \cdot Al_2O_3 \cdot 4.0-6.0SiO_2 \cdot 6H_2O$, where R is



Some zeolites possess sorption properties close to those of small-pore zeolites, even when they have pore openings exceeding 0.45 nm. This is due to blockage of pores by large cations or structural dislocations. Offretite, zeolite T, ZSM-34, and clinoptilolite belong to this category.

Offretite is very closely related to erionite, but presents two important differences. The first one is that the D6R unit's layer sequence is AABAAB. The second one is that the cancrinite cages are no longer rotated by 60° with respect to one another as in erionite. This results in the formation of large channels with a free diameter of about 0.65 nm.¹² Thus, offretite has a complex porous structure that can be understood as the composition of two pore structures: one similar to erionite and another one with large pore openings. Few dislocations or obstructions suffice to prevent access to the wide channels. For example, when offretite is synthesized in the presence of Me_4NOH , to obtain tetramethylammonium (TMA)-offretite, the bulky molecules of this compound are placed in the large channels preventing even the sorption of linear molecules as n-hexane.¹² The partial substitution of TMA by potassium cations enables the molecular sieve to adsorb n-hexane. The removal of TMA cations by heating or exchange with ammonium cations leads to solids with higher accessibility for bulky molecules such as cyclohexane and m-xylene.^{12,14,15} In other cases, due to the similarity of offretite and erionite, it is possible to have solids in which some portions of the crystal are erionite while others consist of offretite. The erionite-offretite intergrowth leads to the obstruction of the large channels. Zeolite T and ZSM-34 are examples of this.

Zeolite T has a hexagonal symmetry and its typical formula is $0.3Na_2O \cdot 0.7K_2O \cdot Al_2O_3 \cdot 6.9SiO_2 \cdot 7.2H_2O$. This zeolite is a disordered intergrowth of offretite and erionite. In zeolite T, the more open structure of offretite is interspersed at intervals with the tighter erionite units. In this way, the large pores of offretite are blocked by the 6-rings of erionite. A single unit cell of erionite at the end of the large pore of offretite is enough to have a complete blockage of it. Even though erionite is only a small

portion of zeolite T structure, the erionite cages control the diffusion path by forcing the molecules to pass through the 8-rings.¹⁶

ZSM-34 seems to be another example of offretite-erionite intergrowth. The highest $\text{SiO}_2/\text{Al}_2\text{O}_3$ molar ratio that has been reported for this zeolite is about 15.¹⁷

Clinoptilolite has a monoclinic symmetry and its typical formula is $(\text{Na}_2, \text{K}_2)\text{O} \cdot \text{Al}_2\text{O}_3 \cdot 10\text{SiO}_2 \cdot 8\text{H}_2\text{O}$. Its porous structure may resemble mordenite.^{12,13} The dimensions of its channels are 0.75×0.30 , 0.43×0.33 and 0.31×0.33 nm. However, the apparent pore size of the nondecationized clinoptilolite is close to that of small-pore zeolites. Its pore size can be enlarged by decationization and dealumination.

Silicoaluminophosphates (SAPOs) are a new generation of crystalline microporous molecular sieves. They have been discovered by incorporating Si into the framework of the aluminophosphates (AlPO_4) molecular sieves. Several small-pore SAPO crystals have been synthesized.¹⁸ SAPO-17, SAPO-34 and SAPO-44 have pore openings of about 0.43 nm. SAPO-17 has an erionite-like structure, while SAPO-34 and SAPO-44 have a chabazite-like structure.^{10,19,20}

An interesting fact is that SAPO molecular sieves show mild acidity, while chabazite and erionite are strong acids in the protonic form (see Table 2).

In SAPO crystals the concentration of Brönsted acid sites increases as the Si/Al-ratio is raised. This is the opposite of what is accepted for zeolites. It may be explained on the assumption that a SAPO crystal is obtained by silicon substitution into a

Table 2 Pseudo-first-order rate constants for n-butane cracking on small-pore molecular sieves^{10,19,20}

| Molecular sieve | k_a ($\text{cm}^3/\text{min} \cdot \text{g}$) | Molecular sieve | k_a ($\text{cm}^3/\text{min} \cdot \text{g}$) |
|-----------------|--|-----------------|--|
| SAPO-17 | 0.5 | BeAPO-34 | 3.7 |
| Erionite | 4-5 | CoAPO-34 | 5-15 |
| SAPO-34 | 0.1-3.2 | FeAPO-34 | 0.1-0.6 |
| Chabazite | 7 | MnAPO-34 | 2.5-5.2 |
| SAPO-44 | 1.2-2.4 | BeAPSO-34 | 7.6 |
